1-1-2011

Improved reversible dehydrogenation of 2LiBH4+MgH2 system by introducing Ni nanoparticles

Jianfeng Mao
jm975@uowmail.edu.au

Zaiping Guo
University of Wollongong, zguo@uow.edu.au

Xuebin Yu
xyu@uow.edu.au

Hua-Kun Liu
University of Wollongong, hua@uow.edu.au

Improved reversible dehydrogenation of $2LiBH_4+MgH_2$ system by introducing Ni nanoparticles

Jianfeng Mao
Institute for Superconducting and Electronic Materials, University of Wollongong, Wollongong, New South Wales 2522, Australia

Zaiping Guo[a)]
Institute for Superconducting and Electronic Materials, University of Wollongong, Wollongong, New South Wales 2522, Australia; and School of Mechanical, Materials & Mechatronics Engineering, University of Wollongong, Wollongong, New South Wales 2522, Australia

Xuebin Yu[b)]
Institute for Superconducting and Electronic Materials, University of Wollongong, New South Wales 2522, Australia; and Department of Materials Science, Fudan University, Shanghai 200433, China

Huakun Liu
Institute for Superconducting and Electronic Materials, University of Wollongong, Wollongong, New South Wales 2522, Australia

(Received 29 November 2010; accepted 3 March 2011)

We report that the hydrogen de/resorption of the $2LiBH_4+MgH_2$ system was modified by introducing Ni nanoparticles. Dehydrogenation analysis revealed that the first-step dehydrogenation, i.e., the decomposition of MgH_2, can be significantly promoted by adding a small amount of Ni because of the catalytic effect. However, the improvement of the second-step dehydrogenation, corresponding to the decomposition of $LiBH_4$, needs the addition of a large amount of Ni, resulting in the formation of a Mg–Ni–B ternary alloy. Furthermore, the presence of the Mg–Ni–B ternary alloy allowed an increased reversible H-capacity, in which about 5.3 wt% of hydrogen can be rehydrogenated under 400 °C and 55 bar hydrogen pressure over 10 h, which is higher than that of the pristine $2LiBH_4+MgH_2$ system (4.4 wt%).

I. INTRODUCTION

Along with the increasing demands for cleaner and more environmentally friendly energy, the use of hydrogen as an energy carrier has attracted significant interest because no pollutants are produced when it is burned or used in fuel cells.[1] However, the challenges to the efficient and safe storage of hydrogen have to be overcome before the widespread use of hydrogen as an energy carrier is possible. Storing hydrogen in metal hydrides is very attractive, as they can offer higher volumetric hydrogen densities than compressed hydrogen gas or liquid hydrogen, without using very high pressure containment vessels or cryogenic tanks.[2] A system target of 5.5 wt% hydrogen for automobile fuelling has been set by the U.S. Department of Energy for 2015.[3] Because the transition metallic hydrides cannot store adequate amounts of hydrogen, interest has focused more recently on lightweight element complex hydrides such as alanates (AlH_4^-),[4–6] amides (NH_2^-),[7,8] and borohydrides (BH_4^-).[9,10]

$LiBH_4$ has a high theoretical hydrogen capacity of 18.5 wt%. It was first reported in 1940 by Schlesinger and Brown, and used to be considered as a powerful reducing agent in organic chemistry.[11] Since the important study of $LiBH_4$ as a hydrogen storage material by Züttel et al. in 2002,[9] various investigations, in such areas as structural analysis, study of dehydrogenation/rehydrogenation behaviours, etc., have been undertaken to provide more insights.[11–13] The complete dehydrogenation reaction can be simplified as follows without mention of the possible formation of the intermediate $Li_2B_{12}H_{12}$ species[14–16]:

$$LiBH_4 \rightarrow LiH + B + 3/2H_2 \quad , \qquad (1)$$

$$LiH \rightarrow Li + 1/2H_2 \quad . \qquad (2)$$

Reaction 1 proceeds around 380–600 °C and liberates 13.8 wt% of hydrogen. The second step liberates another 4.7 wt% at above 700 °C. This temperature is high, and hence the desorption of LiH is not considered as useful capacity for onboard hydrogen storage.

It is obvious that $LiBH_4$ is thermodynamically too stable for the hydrogenation/dehydrogenation cycles to

Address all correspondence to these authors.
[a)]e-mail: zguo@uow.edu.au
[b)]e-mail: yuxuebin@fudan.edu.cn
DOI: 10.1557/jmr.2011.72

proceed at practical pressures and temperatures. Pure $LiBH_4$ requires a temperature of over 400 °C for rapid hydrogen release and rigorous conditions of 600 °C and 35 MPa hydrogen pressure for full restoration of the hydride.[10] Various attempts have been undertaken to overcome the kinetic and thermodynamic limitations, and some improvements have been achieved that enhance the dehydrogenation and rehydrogenation properties of $LiBH_4$, such as reducing the particle size, doping with catalysts such as carbon, metals, oxides, and halides, and reacting with metal hydrides or hydride mixtures.[17–23] Among these attempts, one of the most promising has been proposed by Vajo et al.,[24] that $LiBH_4$ can be effectively destabilized by MgH_2, reducing the dehydrogenation temperature of $LiBH_4$ to near 350 °C and allowing complete decomposition below 500 °C. The reaction of $LiBH_4$ with MgH_2 is proposed as follows:

$$2LiBH_4 + MgH_2 \rightarrow 2LiH + MgB_2 + 4H_2 \quad . \quad (3)$$

The reaction enthalpy is 46 kJ/mol H_2, which is much lower than for the decomposition of pure $LiBH_4$ (74 kJ/mol H_2),[13] because of the formation of MgB_2 during dehydrogenation. Also, the reaction is reversible under more moderate conditions, where 8–10 wt% of hydrogen can be reversibly stored from an initial hydrogen pressure of 100 bar, from a temperature as low as 230–250 °C over 10 h in the presence of 2–3 mol% $TiCl_3$. However, the dehydrogenation kinetics is still poor and a temperature as high as 400 °C is required for a reasonable dehydrogenation rate. More importantly, further research reveals that the dehydriding reaction proceeds by a different mechanism, i.e., MgH_2 and $LiBH_4$ decompose individually.[25–27] The reaction is expressed as follows:

$$MgH_2 + 2LiBH_4 \rightarrow 2LiH + Mg + 2B + 4H_2 \quad . \quad (4)$$

At relatively high temperature (>420 °C), Mg will react with LiH to form Li–Mg alloy, but still there is no formation of MgB_2.[25] The reaction is harder to reverse compared with Eq. (3) because the B–B bond is likely to be more stable than the B–Mg bond.[10] It is suggested that low temperature and high hydrogen back pressure ($T \leq 400$ °C and $p(H_2) \geq 3$ bar) should be applied during the dehydrogenation, to avoid the formation of elemental B from the decomposition of $LiBH_4$.[26,27]

Motivated by these considerations, we have focused on catalyst screening, which is expected to not only lower the dehydrogenation temperature of MgH_2 and $LiBH_4$ but also promote the formation of MgB_2 compound. It is well known that Ni and Ni-based compounds are good catalysts for lowering the dehydrogenation temperature and enhancing the sorption kinetics of MgH_2.[28–30] Meanwhile, it has also been well established that the Ni promotes the activation of B–H bonds, and a B–Ni compound, Ni_2B, was identified to form in the $LiBH_4$–Ni composites upon dehydrogenation.[31,32] However, the Ni_2B compound is more difficult than MgB_2 to reversibly hydrogenate. In particular, Li et al.[33] has shown that a ternary magnesium nickel boride together with MgH_2 and LiH can be hydrogenated reversibly, forming $LiBH_4$ and Mg_2NiH_4 under 100 to 160 bar H_2 at temperatures below ~300 °C, suggesting that some other boride compounds may have more advantages in hydrogenating reversibly and forming $[BH_4]^-$ rather than MgB_2. Actually, it has been reported that the dehydrogenation and rehydrogenation of the $LiBH_4$–MgH_2 system can be effectively improved by introducing Al or $LiAlH_4$, because of the formation upon dehydrogenation of a ternary alloy of Al–Mg–B, which was even formed under vacuum below 400 °C.[34,35] Therefore, in the present study, nanosized Ni is introduced to the $LiBH_4$–MgH_2 system by mechanical alloying to improve its hydrogen storage properties through a combination of the catalytic effect and a possible reaction to form the ternary alloy Ni–Mg–B.

II. EXPERIMENTAL

The chemicals MgH_2 (98% purity), $LiBH_4$ (90% purity), and Ni (99.9% purity, <100-nm particle size) were all purchased from Sigma-Aldrich (Sigma-Aldrich Corporation, St. Louis, MO) and used directly without pretreatment. All sample storage and handling were performed in an Ar filled glove box (MBraun Unilab). Two mixtures of $2LiBH_4$–MgH_2–0.5Ni and $2LiBH_4$–MgH_2–0.05Ni were ball milled for 2 h at a rate of 400 rpm in a QM-2SP planetary ball mill (MBraun Group, Garching, Germany). The ball-to-powder ratio was around 30:1. A $2LiBH_4$–MgH_2 mixture was also prepared under the same conditions for comparison (Nanjing University Instrument Plant, Nanjing, China).

The hydrogen desorption/absorption properties were measured in a Sieverts apparatus (Advanced Materials Corporation), where the temperatures and pressures of the sample and the gas reservoirs were monitored and recorded by GrcLV-LabVIEW-based control program software (Advanced Materials Corporation, Pittsburgh, PA) during the sorption process. Temperature programmed dehydrogenation (TPD) curves were determined by volumetric methods (National Instruments Corporation, Austin, TX) starting from vacuum. The temperature was increased from ambient to ~500 °C at 5 °C/min. The hydrogen desorption kinetic measurements were performed at 350 and 400 °C, starting from vacuum. Before the measurement, the sample chamber was filled with hydrogen at 5-MPa pressure and the temperature was then raised to and kept at the desired temperature. Then, the chamber was quickly evacuated before the onset of measurements. The hydrogen absorption measurements were performed at 400 °C and ~5.5 MPa before the sample was

dehydrogenated at 500 °C under dynamic vacuum. Other than specified, the H-capacity was calculated using the weight of the samples containing additives to allow for an evaluation of the practical hydrogen storage property.

Differential scanning calorimetry (DSC) analysis of the dehydrogenation process was carried out on a Mettler Toledo TGA/DSC 1 (Mettler-Toledo International Incorporation, Zürich, Switzerland). About 6 mg of sample was loaded into an alumina crucible in the glove box. The crucible was then placed in a sealed glass bottle to prevent oxidation during transportation from the glove box to the DSC apparatus. An empty alumina crucible was used as the reference material. The samples were heated from room temperature to 500 °C under 1 atm flowing argon atmosphere, and the heating rate was 10 °C /min.

The structural information on various samples was derived from powder x-ray diffraction (XRD, GBC Scientific Equipment Ltd.; Cu KR radiation, GBC Scientific Equipment Ltd., Braeside, Australia) and Fourier transform infrared (FTIR) spectroscopy (Shimadzu Prestige 21, Shimadzu Corporation, Kyoto, Japan, using samples ground with KBr powder and pressed into a sample cup). To avoid oxidation during the XRD measurement, samples were mounted onto a glass slide 1 mm in thickness in the Ar-filled glovebox and sealed with an airtight hood composed of an amorphous tape, which has a broad peak around 2θ of 20°.

III. RESULTS AND DISCUSSION

Figure 1 presents the TPD curves and the differentiated TPD (DTPD) curves for the dehydrogenation of the $2LiBH_4$–MgH_2 (2:1 mol ratio) and $LiBH_4$–MgH_2–Ni composites (2:1:0.5 and 2:1:0.05 mol ratio, respectively). It can be seen that all the samples showed a clear two-step dehydrogenation, which correspond to the decomposition of MgH_2 and $LiBH_4$. For the pure $2LiBH_4$–MgH_2 system, the first hydrogen desorption started at around 350 °C. Further heating led to a second decomposition at 370 °C and a total hydrogen release capacity of 11 wt% was obtained below 500 °C. Meanwhile, two main peaks of hydrogen evolution located at 365 and 435 °C can be observed in the DTPD results. After doping with a small amount of Ni, the $2LiBH_4$–MgH_2–0.05 Ni sample started to release hydrogen at around 310 °C and reached its first maximum release rate at 331 °C, which is 34 °C lower than that of the pure $2LiBH_4$–MgH_2 sample. However, the same peak temperature of 435 °C for the second dehydrogenation is observed, indicating that the second dehydrogenation cannot be improved by doping with a small amount of Ni. Nevertheless, both the first and the second dehydrogenation steps of the MgH_2–$LiBH_4$ system can be significantly improved by doping with an increased Ni content. As shown in Fig. 1, two main dehydrogenation peaks, located at 313 and 410 °C, are observed in the DTPD results for the $2LiBH_4$–MgH_2–0.5Ni sample, which are 52 and 25 °C lower than for the $2LiBH_4$–MgH_2 sample, indicating enhanced dehydrogenation performance. Although increased doping with Ni will lead to a reduction in the total hydrogen capacity, the $2LiBH_4$–MgH_2–0.5Ni sample still has a theoretical hydrogen storage capacity of 8.08 wt%.

The thermal decomposition behavior of $2LiBH_4$–MgH_2–0.5Ni sample, $2LiBH_4$–MgH_2–0.05Ni sample, and $2LiBH_4$–MgH_2 sample, was further investigated by DSC are presented in Fig. 2. Four endothermic peaks were found on the DSC profile for the three samples. These features can be assigned to the phase transition of $LiBH_4$, the melting of $LiBH_4$, the decomposition of MgH_2, and the hydrogen desorption of $LiBH_4$.[36,37] The plot for the three samples shows the same temperature of 124 °C for the phase transition of $LiBH_4$. However, the $2LiBH_4$–MgH_2–0.5Ni sample has the lowest melting point at 278 °C compared with the other samples, which is 15 and 13 °C lower than that of $2LiBH_4$–MgH_2–0.5Ni sample and $2LiBH_4$–MgH_2 sample, respectively. The results indicate that the large addition of Ni can reduce the melting point of $LiBH_4$. It also can be seen that the peak temperature for the

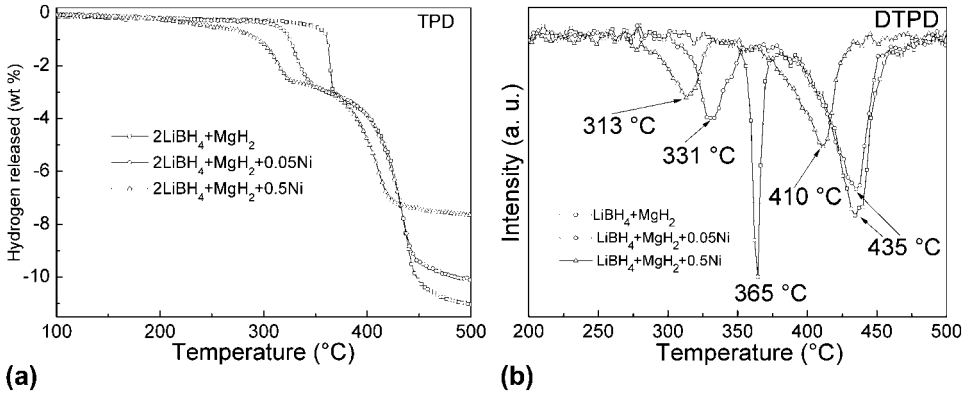

FIG. 1. (a) Temperature-programmed desorption (TPD) and (b) derivative TPD (DTPD) curves of the $2LiBH_4$–MgH_2, $2LiBH_4$–MgH_2–0.05Ni, and $2LiBH_4$–MgH_2–0.5Ni samples after ball milling for 2 h in argon. The heating ramp for all the samples was 5 °C/min.

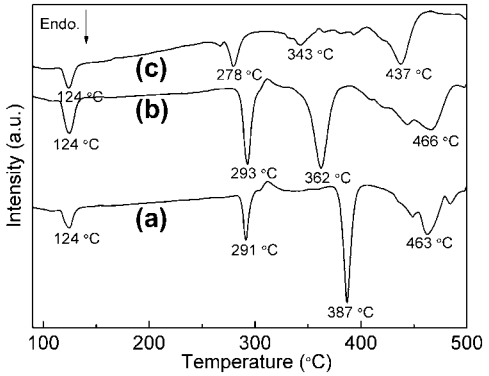

FIG. 2. Differential scanning calorimetry traces for (a) $2LiBH_4$–MgH_2, (b) $2LiBH_4$–MgH_2–0.05Ni, and (c) $2LiBH_4$–MgH_2–0.5Ni samples, with a heating rate of 10 °C/min.

dehydrogenation of MgH_2 and $LiBH_4$ in the $2LiBH_4$–MgH_2 sample is 387 and 463 °C, respectively. After adding a small amount of Ni, the peak temperature for the dehydrogenation of MgH_2 in the $2LiBH_4$–MgH_2–0.05Ni sample is reduced to 362 °C, but the peak temperature for the dehydrogenation of $LiBH_4$ is similar (466 °C). However, the peak temperature for the dehydrogenation of MgH_2 and $LiBH_4$ can be reduced to 343 and 437 °C, respectively, when adding a large amount of Ni ($2LiBH_4$–MgH_2–0.5Ni sample). These results agree well with the TPD results (Fig. 1) and further confirm the effect of Ni on the $LiBH_4$–MgH_2 system. However, the peak temperature for the decomposition in the DSC is slightly higher than that in the TPD (Fig. 1). These differences may result from the fact that the dehydrogenation measurement was run under different conditions in these two cases. The DSC measurement was conducted under 1 atm argon flow with a 10 °C/min heating rate, whereas the TPD measurement was started from 0.1 atm vacuum with a 5 °C/min heating rate. Obviously, the onset decomposition temperature will shift to a higher value when the heating rate increases from 5 to 10 °C/min. On the other hand, the low pressure environment is favorable for the hydrogen release reaction, resulting in the reduced decomposition temperature.

The fact that the first-step dehydrogenation (MgH_2) can be enhanced by doping with a small amount of Ni, whereas the second-step dehydrogenation ($LiBH_4$) is only enhanced by doping with a large amount of Ni, indicates the different mechanisms involved. For understanding well the role of Ni and the possible chemical reactions occurring in the dehydrogenation process of the $LiBH_4$–MgH_2 system, XRD was carried out on the $2LiBH_4$–MgH_2–0.5Ni sample and on the reaction products. Figure 3(a) shows the XRD patterns of the as-prepared $2LiBH_4$–MgH_2–0.5Ni sample before and after heating to 330 and 500 °C, respectively. The dehydrogenation products of the $2LiBH_4$–MgH_2 and $2LiBH_4$–MgH_2–0.05Ni samples after heating to 500 °C were also examined for comparison. Clearly, MgH_2, $LiBH_4$, and Ni phases are detected in the as-milled sample, and no new reaction products can be found, suggesting a physical mixture during ball milling. After heating to 330 °C, the MgH_2 phase disappears and magnesium metal is formed. The $LiBH_4$ phases are still present and no other Mg or B containing phases were detected, indicating that the hydrogen release from the composite below 330 °C is due to the decomposition of MgH_2. Ni phases are also observed after heating to 330 °C, and no additional peaks corresponding to the Mg_2Ni phase were observed, indicating that the enhancement of the first-step dehydrogenation can be attributed to the catalytic effect of nano-Ni, which is highly active in decreasing the activation energy of MgH_2 for hydrogen desorption by surface activation, as reported previously.[29] On further heating to 500 °C, $LiBH_4$ disappeared and LiH phase was observed, indicating that the system is fully dehydrogenated at 500 °C, as the boron phase in dehydrogenated samples of $LiBH_4$-relevant samples is usually amorphous,[22] agreeing well with the TPD results (Fig. 1). Meanwhile, in addition to some traces of Mg or Li–Mg alloy (with Li–Mg alloy and Mg peaks overlapping in the XRD patterns), many new peaks were appeared along with the disappearance of the Ni phase, which can be identified to a new phase of Mg–Ni–B alloy. The Mg–Ni–B phase is quite comparable with $MgNi_{2.5}B_2$ in the database, but it is hard to confirm its nature because of the relatively low content of Ni and because magnesium nickel borides always have a hexagonal crystal structure with similar lattice constants, as previously reported.[33,38] Some traces of the new Mg–Ni–B alloy were also observed in the case of $2LiBH_4$–MgH_2–0.05Ni sample after dehydrogenated at 500 °C. However, the main dehydrogenation products are Mg or Li–Mg, as well as some LiH and MgB_2 [Fig. 3(b)]. As is known, the boron phase in the dehydrogenated samples of $LiBH_4$-relevant is usually amorphous and therefore can not be detected by means of XRD.[22] Similar products corresponding to Mg or Li–Mg, as well as some LiH and MgB_2 were also identified in $2LiBH_4$–MgH_2 sample after dehydrogenated at 500 °C. The observed MgH_2 phase in the dehydrogenated state of $2LiBH_4$–MgH_2 or $2LiBH_4$–MgH_2–0.05Ni sample is probably from the hydrogenation of Mg or Li–Mg during the temperature of 500 °C cooling down to room temperature because about 1 bar hydrogen pressure was observed in the vessel after dehydrogenated at 500 °C. The results indicate that the main dehydrogenation products at 500 °C for the $2LiBH_4$–MgH_2–0.5Ni sample are Mg–Ni–B ternary alloy, LiH and some Mg or Li–Mg, which are totally different from the cases of the $2LiBH_4$–MgH_2 or $2LiBH_4$–MgH_2–0.05Ni samples, for which the main dehydrogenation products are Mg or Li–Mg, B, LiH, and some MgB_2 [Fig. 3(b)]. The different dehydrogenation products suggest different dehydrogenation pathways. In the case of $2LiBH_4$–MgH_2–0.5Ni, an interaction among the Mg, $LiBH_4$ or B, and the Ni occurred during heating, resulting in the formation of the

Mg–Ni–B ternary alloy. In contrast, the interaction of MgH_2 with $LiBH_4$ in the $2LiBH_4$–MgH_2 and $2LiBH_4$–MgH_2–0.05Ni samples is low because B and Mg or Li–Mg were mainly generated upon dehydrogenation.

To judge the storage capacity and kinetics of Ni-modified $LiBH_4$–MgH_2 system at constant temperature. Isothermal dehydrogenation studies were further carried out for the $2LiBH_4$–MgH_2–0.5Ni samples at 350 and 400 °C, as shown in Fig. 4. The $2LiBH_4$–MgH_2 sample is also examined under the same conditions for comparison. Obviously, both the samples show two stages in the dehydriding process at 350 and 400 °C: fast dehydriding in the first short period, corresponding to the decomposition of MgH_2, and slow dehydriding thereafter, which may be attributed to the dehydrogenation of $LiBH_4$. The results agree well with the TPD and DSC results (Figs. 1 and 2). At 350 °C, the hydrogen released is mainly due to the decomposition of MgH_2 in both the $2LiBH_4$–MgH_2–0.5Ni and the $2LiBH_4$–MgH_2 samples, with 3 wt% hydrogen released within 6.3 min in the former, but 15 min is required for the latter to release the same amount of hydrogen under the same conditions, indicating the significant enhancement of the first dehydrogenation. However, the second stage dehydrogenation in both the $2LiBH_4$–MgH_2–0.5Ni and $2LiBH_4$–MgH_2 samples, corresponding to the decomposition of $LiBH_4$, is very slow, which is not completed even after 10 h. At 400 °C, the first dehydrogenation for the $2LiBH_4$–MgH_2–0.5Ni sample is a little faster than for the $2LiBH_4$–MgH_2, which may be due to the fact that 400 °C is over the decomposition temperature of MgH_2 in both samples, resulting in their fast kinetics. However, the second dehydrogenation of $2LiBH_4$–MgH_2–0.5Ni is much faster than that of the $2LiBH_4$–MgH_2. For example, 6.1 wt% hydrogen can be released within 30 min in the former case, which is 1 wt% higher than in the latter case. Meanwhile, the saturated dehydrogenation process for the $2LiBH_4$–MgH_2–0.5Ni sample can be limited to within 55 min, whereas 167 min is required for the $2LiBH_4$–MgH_2. These results further confirmed the significant improvement because of the addition of Ni on the dehydrogenation of the $LiBH_4$–MgH_2 system.

The rehydrogenation of the decomposed $2LiBH_4$–MgH_2–0.5Ni was further investigated under ~55 bar of H_2 at 400 °C for 10 h as compared with the pure $2LiBH_4$–MgH_2 system. Figure 5(a) shows the isothermal rehydrogenation kinetics of both samples as a function of time. A hydrogen capacity of ~4.37 wt% could be achieved after 10 h in the case of $2LiBH_4$–MgH_2, whereas the $2LiBH_4$–

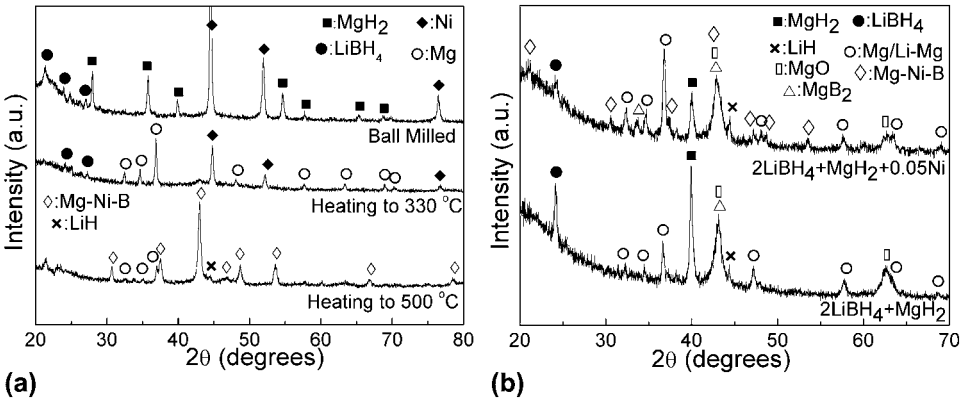

FIG. 3. X-ray diffraction (XRD) patterns of (a) the $2LiBH_4$–MgH_2–0.5Ni sample after ball milling for 2 h and the milled sample after heating to 330 and 500 °C, respectively; and (b) the $2LiBH_4$–MgH_2 and $2LiBH_4$–MgH_2–0.05Ni samples after heating to 500 °C, respectively.

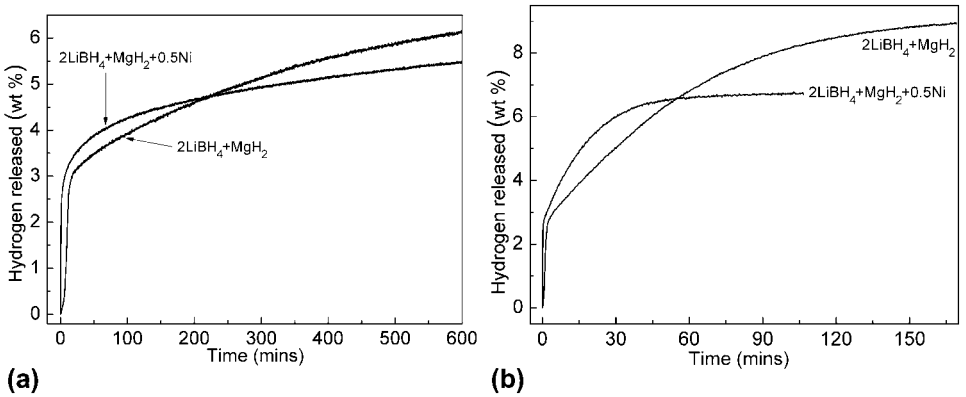

FIG. 4. Hydrogen desorption curves of $2LiBH_4$–MgH_2 and $2LiBH_4$–MgH_2–0.5Ni samples at (a) 350 and (b) 400 °C, respectively.

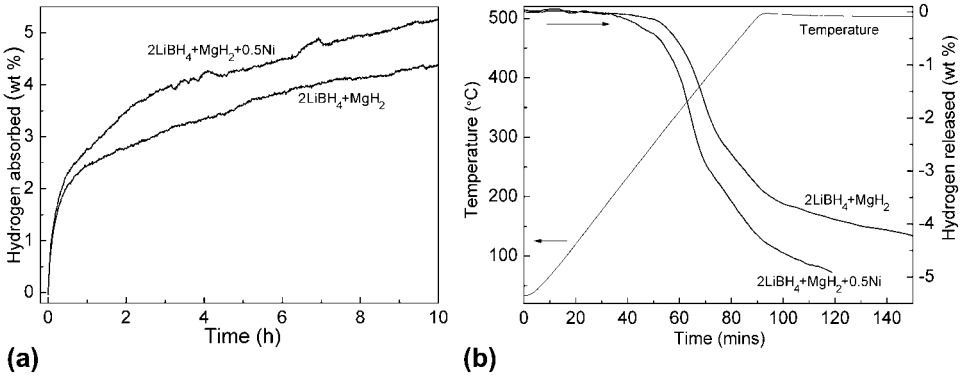

FIG. 5. (a) Isothermal rehydrogenation kinetics of $2LiBH_4$–MgH_2 and $2LiBH_4$–MgH_2–0.5Ni samples under an initial hydrogen pressure of 55 bar and at 400 °C. (b) Comparison of the TPD curves for the first rehydrogenation of the $2LiBH_4$–MgH_2 and $2LiBH_4$–MgH_2–0.5Ni samples.

MgH_2–0.5Ni sample delivered a rehydrogenation capacity of 5.25 wt% under the same conditions. Note that the rechargeable theoretical H-capacity was actually 7.46 wt% in the $2LiBH_4$–MgH_2–0.5Ni sample when excluding the weight of Ni, indicating a much higher reversible rate in $2LiBH_4$–MgH_2–0.5Ni than that for the pure $2LiBH_4$–MgH_2 sample. These results indicate that the rehydrogenation of the $LiBH_4$–MgH_2 system was also significantly improved through adding Ni nanoparticles. The TPD curves for the $2LiBH_4$–MgH_2 and $2LiBH_4$–MgH_2–0.5Ni samples after rehydrogenation are shown in Fig. 5(b). It can be seen that the released hydrogen capacity was 4.22 wt% in the $2LiBH_4$–MgH_2 sample. As expected, more hydrogen was released in the $2LiBH_4$–MgH_2–0.5Ni sample (4.92 wt%). These results are in good agreement with the rehydrogenation kinetic measurements shown in Fig. 5(a), except for a slight decrease on the capacity, which may be due to the fact that the dehydrogenation is not completed below 500 °C.

To determine the rehydrogenation products, XRD and FTIR measurements were carried out. Figure 6 shows the XRD patterns for the $2LiBH_4$–MgH_2–0.5Ni sample after rehydrogenated at 5.5 MPa and 400 °C for 10 h. Clearly, the diffraction from MgH_2 can be seen, although the intensity is low. However, no apparent peaks corresponding to $LiBH_4$ can be identified because of the present high background at around 2θ of 20° generated by the cover tape that is used to cover the sample to avoid the possible oxidation and moisture. Another concern is that the reformed $LiBH_4$ is possible to be amorphous or disorder state, because the typical feature of $[BH_4]$ group in the rehydrogenated state is clearly detected by FTIR spectrum (Fig. 7). However, the recombination of borohydride is obviously incomplete under these conditions because such phases as LiH and Mg–Ni–B phases still remained in the rehydrogenated sample. The formation of MgH_2 may be from the hydrogenation of Mg. However, no Mg_2NiH_4 phase was observed in the XRD patterns, although there are several unidentified peaks at 41.4, 45.4, and 46°. Meanwhile, the typical feature of Mg_2NiH_4 is also not

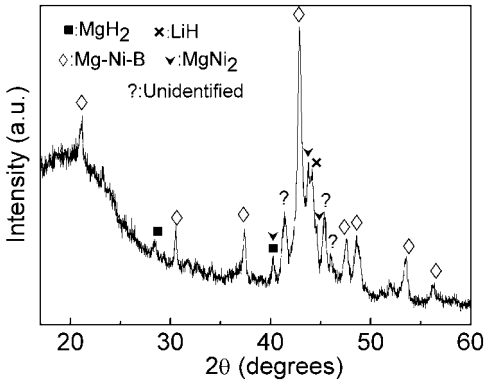

FIG. 6. XRD patterns for the as-dehydrogenated products of $2LiBH_4$–MgH_2–0.5Ni sample after rehydrogenation at 55 bar and 400 °C for 10 h.

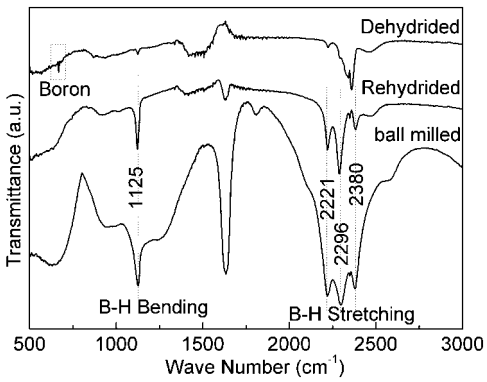

FIG. 7. Fourier transform infrared spectra for the as-milled $2LiBH_4$–MgH_2–0.5Ni sample before and after dehydrogenation at 500 °C and the dehydrogenated products after rehydrogenation at 55 bar and 400 °C for 10 h.

detected by FTIR spectrum (Fig. 7). In contrast, a new phase $MgNi_2$ was formed along with the weakened peaks of Mg–Ni–B ternary alloy. The $MgNi_2$ alloy has been reported to be extremely stable and cannot form hydrides under conventional hydrogenation conditions.[39,40] It has also been reported by Li at el.[33] that Mg_2NiH_4 can not be formed in their rehydrogenated $MgNi_{2.5}B_2$/LiH sample but can be formed in their rehydrogenated $MgNi_{2.5}B_2$/LiH/

MgH_2 sample. In this regard, it is possible that the amount of Ni addition in the $LiBH_4$–MgH_2 system will affect the recovery of MgH_2 or Mg_2NiH_4. We believe therefore that the optimization of Ni amount will be certainly helpful for the full reversibility of the $LiBH_4$–MgH_2–Ni composite. FTIR spectra were further conducted on the $2LiBH_4$–MgH_2–0.5Ni sample to identify the rehydrogenated products, as shown in Fig. 7. Clearly, the typical features of the $[BH_4]$ group can be observed in the spectrum for the as-prepared sample, where the B–H bending vibration (~1125 cm^{-1}) and B–H stretching vibration (2221, 2296, and 2380 cm^{-1}) were detected.[37,41] After dehydrogenation, the peaks corresponding to B–H bond have almost disappeared, in addition, a characterized vibration signal corresponding to boron can be detected in the infrared spectrum.[34] It indicates that the addition of 0.5Ni to the MgH_2 + $2LiBH_4$ material is still not enough to fully transmit the B element to Mg–Ni–B ternary alloy. After rehydrogenation, still no characterized vibration signal corresponding to the Mg_2NiH_4 can be detected.[33] However, The vibration signal corresponding to the B–H bond was clearly detected, which confirmed the formation of borohydride anions.

This study experimentally demonstrates that Ni metal nanoparticles are active toward the reversible dehydrogenation reactions of MgH_2 + $2LiBH_4$ material. Unlike the previous study that the transition metals or transition metal halides are normally introduced just as catalyst.[42,43] In this work, the nano-Ni is introduced not only as a catalyst in catalyzing the decomposition of MgH_2 but also as an additive, which is totally involved into the decomposition of $LiBH_4$, resulting the formation of Mg–Ni–B ternary alloy. For example, the presence of nano-Ni in $2LiBH_4$–MgH_2–0.5Ni sample will firstly catalyze the dehydrogenation of MgH_2. Then the presence of Ni and Mg will destabilize the decomposition of $LiBH_4$ through generating Mg–Ni–B ternary alloy, which changes the de/rehydrogenation pathway of $LiBH_4$, thus improving the kinetics and thermodynamics of the reactions. This finding offers a potential approach for overcoming the kinetic and thermodynamic limitation of $LiBH_4$–MgH_2 system. For example, there are numerous metal nanoparticles such as Ti, Nb, Fe, Co, and etc., which have been reported to be active in catalyzing the dehydrogenation of MgH_2[28,30] It is also possible to form Mg–M–B ternary alloy (M=Ti, Nb, Fe, Co, and so on). Currently, our ongoing efforts focus on the optimization of the composition of $LiBH_4$, MgH_2, and Ni and the rehydriding conditions to reach a full reversibility.

IV. CONCLUSION

In summary, nanosized Ni was used to prepare $LiBH_4$–MgH_2–Ni (2:1:0.5 and 2:1:0.05 mol ratio) composites for enhancing the hydrogen de/resorption performances of the $LiBH_4$–MgH_2 (2:1 mol ratio) system. The first-step dehydrogenation (MgH_2) was significantly promoted in both the $2LiBH_4$-MgH_2–0.05Ni and the $2LiBH_4$–MgH_2–0.5Ni composites because of the catalytic effect of nano-Ni, but the second-step dehydrogenation ($LiBH_4$) is only enhanced in the latter. A higher reversible capacity was also observed in the case of $LiBH_4$–MgH_2–0.5Ni in which ~5.3 wt% hydrogen can be reversibly stored when the sample is held under 400 °C and 55 bar hydrogen pressure for 10 h, which is higher than for the $2LiBH_4$–MgH_2 sample (4.4 wt%). The formation of borohydride anions was confirmed by FTIR in the rehydrogenated sample. XRD analysis indicates that the Mg–Ni–B ternary alloy formed upon dehydrogenation in the case of $2LiBH_4$–MgH_2–0.5Ni composites, which is different compared with the $2LiBH_4$–MgH_2 and $2LiBH_4$–MgH_2–0.05Ni samples, where Mg or Li–Mg alloy and B were mainly generated upon dehydrogenation. The formation of Mg–Ni–B ternary alloy may play a crucial role in enhancing the hydrogen de/absorption of $2LiBH_4$–MgH_2 system by changing the original dehydrogenation/rehydrogenation pathway.

ACKNOWLEDGMENTS

Financial support from Australian Research Council Discovery project (DP0878661) and the National Natural Science Foundation of China (Grant No. 51071047) are gratefully acknowledged.

REFERENCES

1. L. Schlapbach and A. Züttel: Hydrogen-storage materials for mobile applications. *Nature* **414**, 353 (2001).
2. W. Grochala and P.P. Edwards: Thermal decomposition of the non-interstitial hydrides for the storage and production of hydrogen. *Chem. Rev.* **104**, 1283 (2004).
3. DOE targets for onboard hydrogen storage systems for light-duty vehicles: Available at http://www1.eere.energy.gov/hydrogenandfuelcells/storage/pdfs/targets_onboard_hydro_storage.pdf. (Jan. 4, 2004).
4. B. Bogdanović and M. Schwickardi: Ti-doped alkali metal aluminium hydrides as potential novel reversible hydrogen-storage materials. *J. Alloy. Comp.* **253**, 1 (1997).
5. J. Chen, N. Kuriyama, Q. Xu, H.T. Takeshita, and T. Sakai: Reversible hydrogen storage via titanium-catalyzed $LiAlH_4$ and Li_3AlH_6. *J. Phys. Chem. B* **105**, 11214 (2001).
6. J.F. Mao, X.B. Yu, Z.P. Guo, C.K. Poh, H.K. Liu, Z. Wu, and J. Ni: Improvement of the $LiAlH_4$-$NaBH_4$ system for reversible hydrogen storage. *J. Phys. Chem. C* **113**, 10813 (2009).
7. P. Chen, Z.T. Xiong, J. Luo, J. Lin, and K. Tan: Interaction of hydrogen with metal nitrides and imides. *Nature* **420**, 302 (2002).
8. W.F. Luo: ($LiNH_2$-MgH_2): A viable hydrogen storage system. *J. Alloy. Comp.* **381**, 284 (2004).
9. A. Züttel, S. Rentsch, P. Fischer, P. Wenger, P. Sudan, Ph. Mauron, and C. Emmenegger: Hydrogen storage properties of $LiBH_4$. *J. Alloy. Comp.* **356**, 515 (2003).
10. S. Orimo, Y. Nakamori, G. Kitahara, K. Miwa, N. Ohba, S. Towata, and A. Züttel: Dehydriding and rehydriding reactions of $LiBH_4$. *J. Alloy. Comp.* **404**, 427 (2005).
11. L. Laversenne and B. Bonnetot: Hydrogen storage using borohydrides. *Ann. Chim. Sci. Mat.* **30**, 495 (2005).

12. Y. Nakamori, K. Miwa, A. Ninomiya, H. Li, N. Ohba, S.I. Towata, A. Züttel, and S. Orimo: Correlation between thermodynamical stabilities of metal borohydrides and cation electronegativites: First-principles calculations and experiments. *Phys. Rev. B* **74**, 045126 (2006).
13. P. Mauron, F. Buchter, O. Friedrichs, A. Remhof, M. Bielmann, N.Z. Christoph, and A. Züttel: Stability and reversibility of $LiBH_4$. *J. Phys. Chem. B* **112**, 906 (2008).
14. S. Orimo, Y. Nakamori, N. Ohba, K. Miwa, M. Aoki, S. Towata, and A. Züttel: Experimental studies on intermediate compound of $LiBH_4$. *Appl. Phys. Lett.* **89**, 021920 (2006).
15. J.-H. Her, M. Yousufuddin, W. Zhou, S.S. Jalisatgi, J.G. Kulleck, J.A. Zan, S.-J. Hwang, R.C. Bowman, and T.J. Udovic: Crystal structure of $Li_2B_{12}H_{12}$: A possible intermediate species in the decomposition of $LiBH_4$. *Inorg. Chem.* **47**, 9757 (2008).
16. S.-J. Hwang, R.C. Bowman, J.W. Reiter Jr., J. Rijssenbeek, G.L. Soloveichik, J.-C. Zhao, H. Kabbour, and C.C. Ahn: NMR confirmation for formation of $[B_{12}H_{12}]^{2-}$ complexes during hydrogen desorption from metal borohydrides. *J. Phys. Chem. C* **112**, 3164 (2008).
17. Y. Zhang, W.S. Zhang, A.Q. Wang, L.X. Sun, M.Q. Fan, H.L. Chu, J.C. Sun, and T. Zhang: $LiBH_4$ nanoparticles supported by disordered mesoporous carbon: Hydrogen storage performances and destabilization mechanisms. *Int. J. Hydrogen Energy* **32**, 3976 (2007).
18. A.F. Gross, J.J. Vajo, S.L. Van Atta, and G.L. Olson: Enhanced hydrogen storage kinetics of $LiBH_4$ in nanoporous carbon scaffolds. *J. Phys. Chem. C* **112**, 5651 (2008).
19. X.B. Yu, Z. Wu, Q. Chen, Z. Li, B. Weng, and T. Huang: Improved hydrogen storage properties of $LiBH_4$ destabilized by carbon. *Appl. Phys. Lett.* **90**, 034106 (2007).
20. J. Yang, A. Sudik, and C. Wolverton: Destabilizing $LiBH_4$ with a metal (M = Mg, Al, Ti, V, Cr, or Sc) or metal hydride (MH_2= MgH_2, TiH_2, or CaH_2). *J. Phys. Chem. C* **111**, 19134 (2007).
21. X.B. Yu, D.M. Grant, and G.S. Walker: Low-Temperature dehydrogenation of $LiBH_4$ through destabilization with TiO_2. *J. Phys. Chem. C* **112**, 11059 (2008).
22. M. Au and A. Jurgensen: Modified lithium borohydrides for reversible hydrogen storage. *J. Phys. Chem. B* **110**, 7062 (2006).
23. M. Au, A. Jurgensen, W. Spencer, D. Anton, F.E. Pinkerton, S. Hwang, C. Kim, and R. Bowman: Stability and reversibility of lithium borohydrides doped by metal halides and hydrides. *J. Phys. Chem. C* **112**, 18661 (2008).
24. J.J. Vajo, S.L. Skeith, and F. Mertens: Reversible storage of hydrogen in destabilized $LiBH_4$. *J. Phys. Chem. B* **109**, 3719 (2005).
25. X.B. Yu, D.M. Grant, and G.S. Walker: A new dehydrogenation mechanism for reversible multicomponent borohydride systems—The role of Li–Mg alloys. *Chem. Commun.* **37**, 3906 (2006).
26. F.E. Pinkerton, M.S. Meyer, G.P. Meisner, M.P. Balogh, and J.J. Vajo: Phase boundaries and reversibility of $LiBH_4/MgH_2$ hydrogen storage material. *J. Phys. Chem. C* **111**, 12881 (2007).
27. U. Bösenberg, D.B. Ravnsbæk, H. Hagemann, V.D. Anna, C.B. Minella, C. Pistidda, W.V. Beek, T.R. Jensen, R. Bormann, and M. Dornheim: Pressure and temperature influence on the desorption pathway of the $LiBH_4$−MgH_2 composite system. *J. Phys. Chem. C* **114**, 15212 (2010).
28. C.X. Shang, M. Bououdina, Y. Song, and Z.X. Guo: Mechanical alloying and electronic simulations of (MgH_2 + M) systems (M-Al, Ti, Fe, Ni, Cu and Nb) for hydrogen storage. *Int. J. Hydrogen Energy* **29**, 73 (2004).
29. N. Hanada, T. Ichikawa, and H. Fujii: Catalytic effect of nanoparticle 3d-transition metals on hydrogen storage properties in magnesium hydride MgH_2 prepared by mechanical milling. *J. Phys. Chem. B* **109**, 7188 (2005).
30. J.F. Mao, Z.P. Guo, X.B. Yu, H.K. Liu, Z. Wu, and J. Ni: Enhanced hydrogen sorption properties of Ni and Co-catalyzed MgH_2. *Int. J. Hydrogen Energy* **35**, 4569 (2010).
31. G.L. Xia, Y.H. Guo, Z. Wu, and X.B. Yu: Enhanced hydrogen storage performance of $LiBH_4$-Ni composite. *J. Alloy. Comp.* **479**, 545 (2009).
32. Z.Z. Fang, X.D. Kang, P. Wang, and H.M. Cheng: Improved reversible dehydrogenation of lithium borohydride by milling with as-prepared single-walled carbon nanotubes. *J. Phys. Chem. C* **112**, 17023 (2008).
33. W. Li, J.J. Vajo, R.C. Cumberland, P. Liu, S.J. Hwang, C. Kim, and R.C. Bowman: Hydrogenation of magnesium nickel boride for reversible hydrogen storage. *J. Phys. Chem. Lett.* **1**, 69 (2010).
34. Y. Zhang, Q.F. Tian, H.L. Chu, J. Zhang, L.X. Sun, J.C. Sun, and Z.S. Wen: Hydrogen de/resorption properties of the $LiBH_4$-MgH_2-Al system. *J. Phys. Chem. C* **113**, 21964 (2009).
35. J.F. Mao, Z.P. Guo, H.Y. Leng, Z. Wu, Y.H. Guo, X.B. Yu, and H.K. Liu: Reversible hydrogen storage in destabilized $LiAlH_4$-MgH_2-$LiBH_4$ ternary-hydride system doped with TiF_3. *J. Phys. Chem. C* **114**, 11643 (2010).
36. T. Nakagawa, T. Ichikawa, N. Hanada, Y. Kojima, and H. Fujii: Thermal analysis on the Li-Mg-B-H systems. *J. Alloy. Comp.* **446**, 306 (2007).
37. L. Zeng, H. Miyaoka, T. Ichikawa, and Y. Kojima: Superior hydrogen exchange effect in the MgH_2-$LiBH_4$ system. *J. Phys. Chem. C* **114**, 13132 (2010).
38. P. Manfrinetti, M. Pani, S.K. Dhar, and R. Kulkarni: Structure, transport and magnetic properties of $MgNi_3B_2$. *J. Alloy. Comp.* **428**, 94 (2007).
39. J.J. Reilly and R.H. Wiswall: Reaction of hydrogen with alloys of magnesium and nickel and the formation of Mg_2NiH_4. *Inorg. Chem.* **7**, 2254 (1968).
40. A. Kamegawa, Y. Goto, R. Kataoka, H. Takamura, and M. Okada: High-pressure synthesis of novel compounds in an Mg–Ni system. *Renewable Energy* **33**, 221 (2008).
41. L.L. Shaw, X.F. Wan, J.Z. Hu, J.H. Hwak, and Z.G. Yang: Solid-state hydriding mechanism in the $LiBH_4$ + MgH_2 system. *J. Phys. Chem. C* **114**, 8089 (2010).
42. K. Crosby, X.F. Wan, and L.L. Shaw: Improving solid-state hydriding and dehydriding properties of the $LiBH_4$ plus MgH_2 system with the addition of Mn and V dopants. *J. Power Sources* **195**, 7380 (2010).
43. U. Bösenberg, J.W. Kim, D. Gosslar, N. Eigen, T.R. Jensen, J.M. Bellosta von Colbe, Y. Zhou, M. Dahms, D.H. Kim, R. Günther, Y.W. Cho, K.H. Oh, T. Klassen, R. Bormann, and M. Dornheim: Role of additives in $LiBH_4$–MgH_2 reactive hydride composites for sorption kinetics. *Acta Mater.* **58**, 3381 (2010).